China-Japan collaboration workshop on
"Nuclear mass and life for unravelling mysteries of r-process"

Deformed Halo Structure in ^{22}C with Deformed Relativistic Hartree-Bogoliubov Model

Xiang-Xiang Sun

ITP, CAS

06-27-2017

Supervisor: Shan-Gui Zhou

Center for Computational Sciences, University of Tsukuba, Tsukuba 305-8577, Japan

OUTLINE

Background

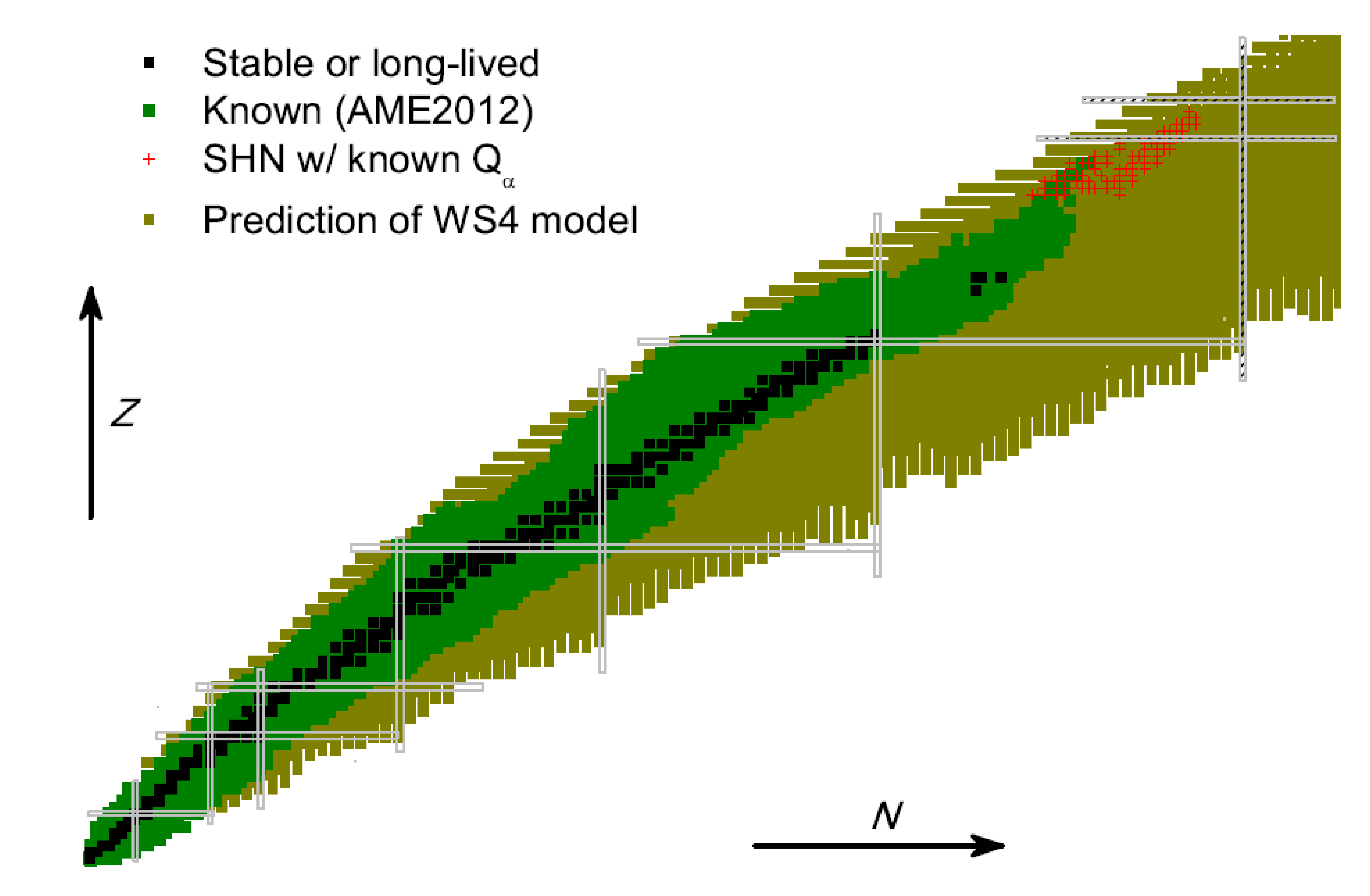

Shan-Gui Zhou, PoS-INPC2016, 373 (2017)

Background

Background

- In carbon isotopes, $^{15}\mathrm{C}$, $^{19}\mathrm{C}$ and $^{22}\mathrm{C}$ are halo nuclei, $^{22}\mathrm{C}$ exhibits a Borromean structure.

- Isao Tanihata, Herve Savajols and Rituparna Kanungo, Prog. Part. Nucl. Phys. **68**, 215-313 (2013);
- Y. Togano et al., Phys. Lett. B **761**, 412-418 (2016);
- M.V. Zhukov et al., Phys. Rep. **213**, 151-199 (1993).

Background

- In carbon isotopes, $^{15}\mathrm{C}$, $^{19}\mathrm{C}$ and $^{22}\mathrm{C}$ are halo nuclei, $^{22}\mathrm{C}$ exhibits a Borromean structure.
  - Isao Tanihata, Herve Savajols and Rituparna Kanungo, Prog. Part. Nucl. Phys. **68**, 215-313 (2013);
  - Y. Togano et al., Phys. Lett. B **761**, 412-418 (2016);
  - M.V. Zhukov et al., Phys. Rep. **213**, 151-199 (1993).
- Experiments about ^{22}C:

Background

- In carbon isotopes, $^{15}\mathrm{C}$, $^{19}\mathrm{C}$ and $^{22}\mathrm{C}$ are halo nuclei, $^{22}\mathrm{C}$ exhibits a Borromean structure.
  - Isao Tanihata, Herve Savajols and Rituparna Kanungo, Prog. Part. Nucl. Phys. **68**, 215-313 (2013);
  - Y. Togano et al., Phys. Lett. B **761**, 412-418 (2016);
  - M.V. Zhukov et al., Phys. Rep. **213**, 151-199 (1993).
- Experiments about ^{22}C:

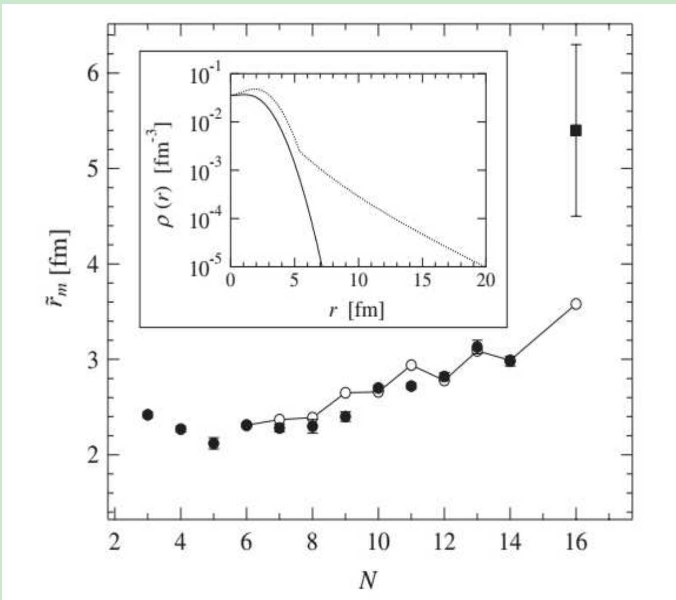

$$R_m = 5.4 \pm 0.9 \text{ fm}$$

K. Tanaka, et al, Phys. Rev. Lett. **104**, 062701 (2010)

Background

- In carbon isotopes, $^{15}\mathrm{C}$, $^{19}\mathrm{C}$ and $^{22}\mathrm{C}$ are halo nuclei, $^{22}\mathrm{C}$ exhibits a Borromean structure.
  - Isao Tanihata, Herve Savajols and Rituparna Kanungo, Prog. Part. Nucl. Phys. **68**, 215-313 (2013);
  - Y. Togano et al., Phys. Lett. B **761**, 412-418 (2016);
  - M.V. Zhukov et al., Phys. Rep. **213**, 151-199 (1993).
- Experiments about ^{22}C:

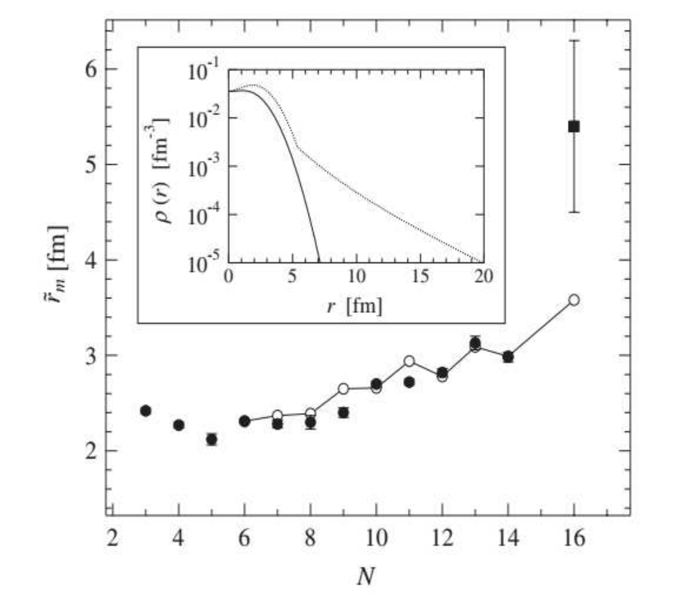

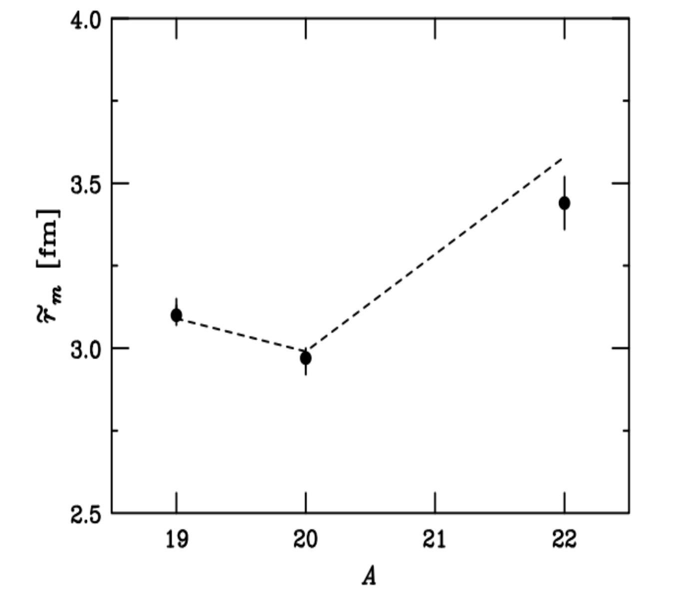

$R_m = 5.4 \pm 0.9$ fm
K. Tanaka, et al, Phys. Rev. Lett. **104**, 062701 (2010)

$R_m = 3.44 \pm 0.08$ fm
Y. Togano, et al, Phys. Lett. B **761**, 412-418 (2016)

The analyzing of those two papers show the valence neutron of ^{22}C is dominated by $2s_{1/2}$.

Background

Background

- Theoretical prediction: three-body model, shell model approach, effective field theory: $2s_{1/2}$.

  - W. Horiuchi and Y. Suzuki, Phys. Rev. C **72**, 034311 (2006); H. T. Fortune and R. Sherr, Phys. Rev. C **85**, 027303 (2012);
  - K. Tanaka, et al, Phys. Rev. Lett. **104**, 062701 (2010); T. Inakura, et al, Phys. Rev. C **89**, 064316 (2014);
  - L. A. Souza, E. Garrido, and T. Frederico,Phys. Rev. C **94**, 064002 (2016).

Background

- Theoretical prediction: three-body model, shell model approach, effective field theory: $2s_{1/2}$.
  - W. Horiuchi and Y. Suzuki, Phys. Rev. C **72**, 034311 (2006); H. T. Fortune and R. Sherr, Phys. Rev. C **85**, 027303 (2012);
  - K. Tanaka, et al, Phys. Rev. Lett. **104**, 062701 (2010); T. Inakura, et al, Phys. Rev. C **89**, 064316 (2014);
  - L. A. Souza, E. Garrido, and T. Frederico,Phys. Rev. C **94**, 064002 (2016).
- Halo nuclei: large spatial distributions, contribution of continuum states and deformation effects. A self-consistent method to describe halo structure: DRHBc model.
  - Jie Meng, Shan-Gui Zhou, J. Phys. G: Nucl. Phys. **42**, 093101 (2015);
  - Jie Meng and Peter Ring, Phys. Rev. Lett. **77**, 3396 (1996); Jie Meng, Nucl. Phys. A **635**, 3 (1998);
  - Shan-Gui Zhou, Jie Meng, Peter Ring, Phys. Rev. C **68**, 034323 (2003);
  - Shan-Gui Zhou, Jie Meng Reter Ring and En-Guang Zhao, Phys. Rev. C **82**, 011301 (2010)(R);
  - Lu-Lu Li, Jie Meng, En-Guang Zhao and Shan-Gui Zhou, Phys. Rev. C **85**, 024312 (2012);

OUTLINE

Covariant density functional theory

- Lagrange density:

$$
\begin{aligned}
\mathcal{L} &= \mathcal{L}_N + \mathcal{L}_\sigma + \mathcal{L}_\omega + \mathcal{L}_\rho + \mathcal{L}_A + \mathcal{L}_I \\
&= \bar{\psi}(i\gamma^\mu\partial_\mu - M)\psi + \frac{1}{2}\partial_\mu\sigma\partial^\mu\sigma - U(\sigma) - g_\sigma\bar{\psi}\sigma\psi \\
&- \frac{1}{4}\Omega_{\mu\nu}\Omega^{\mu\nu} + \frac{1}{2}m_\omega^2\omega_\mu\omega^\mu - g_\omega\bar{\psi}\gamma^\mu\omega_\mu\psi \\
&- \frac{1}{4}\vec{R}_{\mu\nu}\vec{R}^{\mu\nu} + \frac{1}{2}m_\rho^2\vec{\rho}_\mu\vec{\rho}^\mu - g_\rho\bar{\psi}\gamma^\mu\vec{\rho}_\mu\vec{\tau}\psi \\
&- \frac{1}{4}F_{\mu\nu}F^{\mu\nu} - e\bar{\psi}\frac{1-\tau_3}{2}\gamma^\mu A_\mu\psi.
\end{aligned}
$$

$U(\sigma) = \frac{1}{2}m_\sigma^2\sigma^2 + \frac{g_2}{3}\sigma^2 + \frac{g_3}{4}\sigma^4.$

Covariant density functional theory

- Lagrange density:

$$
\begin{aligned}
\mathcal{L} &= \mathcal{L}_N + \mathcal{L}_\sigma + \mathcal{L}_\omega + \mathcal{L}_\rho + \mathcal{L}_A + \mathcal{L}_I \\
&= \bar{\psi}(i\gamma^\mu\partial_\mu - M)\psi + \frac{1}{2}\partial_\mu\sigma\partial^\mu\sigma - U(\sigma) - g_\sigma\bar{\psi}\sigma\psi \\
&- \frac{1}{4}\Omega_{\mu\nu}\Omega^{\mu\nu} + \frac{1}{2}m_\omega^2\omega_\mu\omega^\mu - g_\omega\bar{\psi}\gamma^\mu\omega_\mu\psi \\
&- \frac{1}{4}\vec{R}_{\mu\nu}\vec{R}^{\mu\nu} + \frac{1}{2}m_\rho^2\vec{\rho}_\mu\vec{\rho}^\mu - g_\rho\bar{\psi}\gamma^\mu\vec{\rho}_\mu\vec{\tau}\psi \\
&- \frac{1}{4}F_{\mu\nu}F^{\mu\nu} - e\bar{\psi}\frac{1-\tau_3}{2}\gamma^\mu A_\mu\psi.
\end{aligned}
$$

$U(\sigma) = \frac{1}{2}m_\sigma^2\sigma^2 + \frac{g_2}{3}\sigma^2 + \frac{g_3}{4}\sigma^4.$

Equation of motion (with time reversal invariance):

$$
\begin{aligned}
[-\Delta + \partial_\sigma U(\sigma)] &= -g_\sigma\rho_s; \\
(-\Delta + m_\omega^2)\omega^0 &= g_\omega\rho_\nu; \\
(-\Delta + m_\rho^2)\rho_3^0 &= g_\rho\rho_3; \\
-\Delta A^0 &= e\rho_c;
\end{aligned}
$$

$$(\boldsymbol{\alpha}\cdot\mathbf{p} + \beta(M+S) + V)\psi_i(x) = \varepsilon_i\psi_i(x).$$

Density and current:

$$\rho_s(\mathbf{r}) = \bar{\psi}\psi,\ \rho_\nu(\mathbf{r}) = \bar{\psi}\gamma_\mu\psi,$$

$$\rho_3(\mathbf{r}) = \bar{\psi}\gamma_\mu\tau_3\psi,\ \rho_c(\mathbf{r}) = \bar{\psi}\frac{1-\tau_3}{2}\gamma_\mu\psi.$$

Deformed relativistic Hartree-Bogoliubov model

Deformed relativistic Hartree-Bogoliubov model

- Dirac Hartree-Bogoliubov equation:

$$\int d^3\mathbf{r}' \begin{pmatrix} h_{\rm D}-\lambda & \Delta \\ -\Delta^* & -h_{\rm D}+\lambda \end{pmatrix} \begin{pmatrix} U_k \\ V_K \end{pmatrix} = E_k \begin{pmatrix} U_k \\ V_K \end{pmatrix}.$$

Dirac Hamiltonian: $h_{\rm D}(\mathbf{r},\mathbf{r}') = \boldsymbol{\alpha}\,\mathbf{.}\,\mathbf{p} + V(r) + \beta[M + S(r)]$.

Scalar and vector potential: $S(\mathbf{r}) = g_\sigma \sigma(\mathbf{r})$; $V(\mathbf{r}) = g_\omega \omega^0 + g_\rho \tau_3 \rho^0 + e\frac{1-\tau_3}{2}A^0$.

Deformed relativistic Hartree-Bogoliubov model

- Dirac Hartree-Bogoliubov equation:

$$\int d^3\mathbf{r}' \begin{pmatrix} h_{\mathrm{D}} - \lambda & \Delta \\ -\Delta^* & -h_{\mathrm{D}} + \lambda \end{pmatrix} \begin{pmatrix} U_k \\ V_K \end{pmatrix} = E_k \begin{pmatrix} U_k \\ V_K \end{pmatrix}.$$

  Dirac Hamiltonian: $h_{\mathrm{D}}(\mathbf{r}, \mathbf{r}') = \boldsymbol{\alpha} \cdot \mathbf{p} + V(r) + \beta[M + S(r)]$.
  Scalar and vector potential: $S(\mathbf{r}) = g_\sigma \sigma(\mathbf{r})$; $V(\mathbf{r}) = g_\omega \omega^0 + g_\rho \tau_3 \rho^0 + e\frac{1-\tau_3}{2} A^0$.
- Quasi particle wave function (Dirac spinor) is extended in terms of spherical Dirac spinors,

$$U_k(\mathbf{r}sp) = \sum_{n\kappa} u^{(m)}_{k,(n\kappa)} \phi_{n\kappa m}(\mathbf{r}sp), \quad V_k(\mathbf{r}sp) = \sum_{n\kappa} v^{(m)}_{k,(n\kappa)} \bar{\phi}_{n\kappa m}(\mathbf{r}sp).$$

Deformed relativistic Hartree-Bogoliubov model

- Dirac Hartree-Bogoliubov equation:

$$\int d^3\mathbf{r}' \begin{pmatrix} h_{\mathrm{D}} - \lambda & \Delta \\ -\Delta^* & -h_{\mathrm{D}} + \lambda \end{pmatrix} \begin{pmatrix} U_k \\ V_K \end{pmatrix} = E_k \begin{pmatrix} U_k \\ V_K \end{pmatrix}.$$

Dirac Hamiltonian: $h_{\mathrm{D}}(\mathbf{r}, \mathbf{r}') = \boldsymbol{\alpha} . \mathbf{p} + V(r) + \beta[M + S(r)]$.
Scalar and vector potential: $S(\mathbf{r}) = g_\sigma \sigma(\mathbf{r})$; $V(\mathbf{r}) = g_\omega \omega^0 + g_\rho \tau_3 \rho^0 + e\frac{1-\tau_3}{2} A^0$.

- Quasi particle wave function (Dirac spinor) is extended in terms of spherical Dirac spinors,

$$U_k(\mathbf{r}sp) = \sum_{n\kappa} u_{k,(n\kappa)}^{(m)} \phi_{n\kappa m}(\mathbf{r}sp), \quad V_k(\mathbf{r}sp) = \sum_{n\kappa} v_{k,(n\kappa)}^{(m)} \bar{\phi}_{n\kappa m}(\mathbf{r}sp).$$

- For axially deformed nuclei with spatial reflection symmetry, we represent the potential and densities in terms of Legendre polynomials,

$$f(\mathbf{r}) = \sum_\lambda f_\lambda(r) P_\lambda(\cos\theta), f_\lambda(r) = \frac{2\lambda+1}{2}\int_{-1}^{1} d(\cos\theta) f(\mathbf{r}) P_\lambda(\cos\theta), \lambda = 0, 2, 4...$$

Deformed relativistic Hartree-Bogoliubov model

- Dirac Hartree-Bogoliubov equation:

$$\int d^3\mathbf{r}' \begin{pmatrix} h_{\mathrm{D}} - \lambda & \Delta \\ -\Delta^* & -h_{\mathrm{D}} + \lambda \end{pmatrix} \begin{pmatrix} U_k \\ V_K \end{pmatrix} = E_k \begin{pmatrix} U_k \\ V_K \end{pmatrix}.$$

  Dirac Hamiltonian: $h_{\mathrm{D}}(\mathbf{r},\mathbf{r}') = \boldsymbol{\alpha}\cdot\mathbf{p} + V(r) + \beta[M + S(r)]$.
  Scalar and vector potential: $S(\mathbf{r}) = g_\sigma \sigma(\mathbf{r}); V(\mathbf{r}) = g_\omega \omega^0 + g_\rho \tau_3 \rho^0 + e\frac{1-\tau_3}{2}A^0$.

- Quasi particle wave function (Dirac spinor) is extended in terms of spherical Dirac spinors,

$$U_k(\mathbf{r}sp) = \sum_{n\kappa} u_{k,(n\kappa)}^{(m)} \phi_{n\kappa m}(\mathbf{r}sp), \quad V_k(\mathbf{r}sp) = \sum_{n\kappa} v_{k,(n\kappa)}^{(m)} \bar{\phi}_{n\kappa m}(\mathbf{r}sp).$$

- For axially deformed nuclei with spatial reflection symmetry, we represent the potential and densities in terms of Legendre polynomials,

$$f(\mathbf{r}) = \sum_\lambda f_\lambda(r) P_\lambda(\cos\theta), f_\lambda(r) = \frac{2\lambda+1}{2}\int_{-1}^{1} d(\cos\theta) f(\mathbf{r}) P_\lambda(\cos\theta), \lambda = 0, 2, 4...$$

- Density dependent pairing force of zero range:

$$V^{\mathrm{pp}}(\mathbf{r}_1,\mathbf{r}_2) = \frac{1}{2}V_0(1 - \mathrm{P}^\sigma)\delta(\mathbf{r}_1 - \mathbf{r}_2)\left(1 - \frac{\rho(\mathbf{r}_1)}{\rho_{\mathrm{sat}}}\right).$$

Lulu Li et al, Phys. Rev. C **85**, 024312 (2012).

OUTLINE

Carbon isotopes $^{10-22}$C properties

Fermi level and neutron separation energy are plotted as a function of mass number.

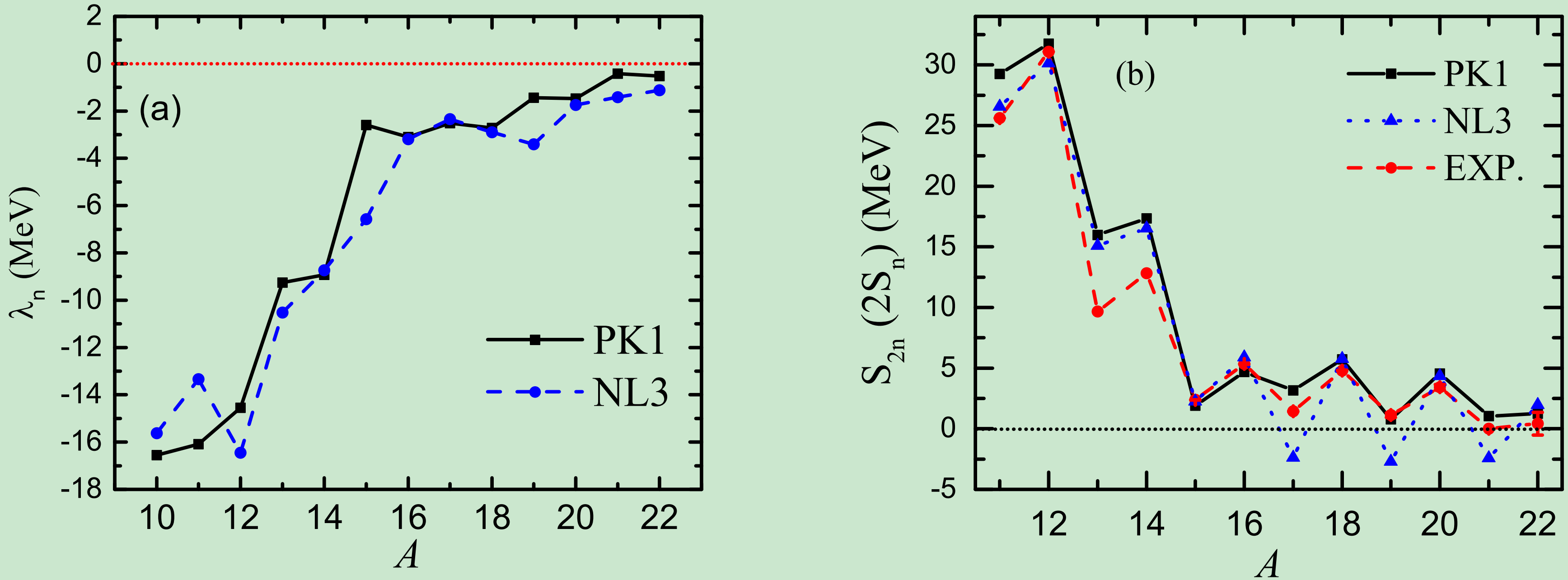

Experimental data are taken from

G. Audi, M. Wang et al. China Physics C **36**, 1287 (2012).

Carbon isotopes $^{10-22}\mathrm{C}$ properties

Root mean square radii $R_{\rm m}$ and proton radii $R_{\rm p}$ are plotted as a function of nucleon number A.

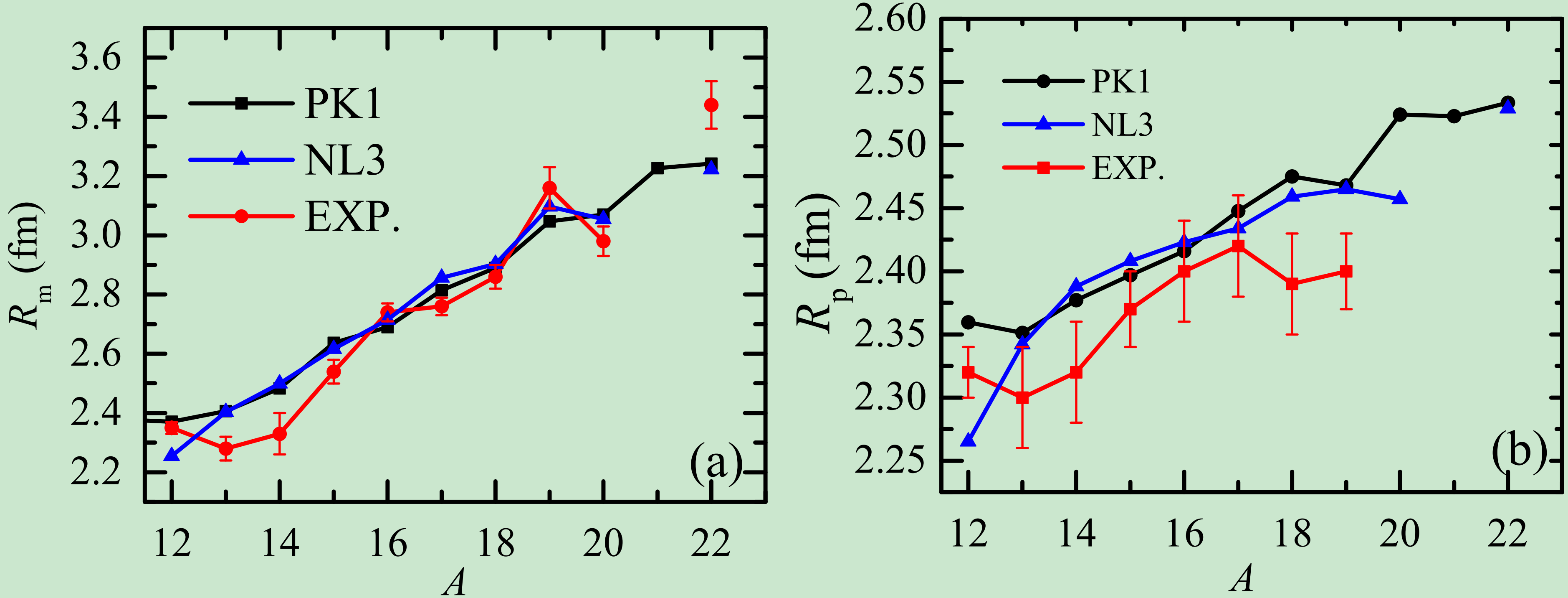

The experimental data are taken from

- R. Kanungo et al., Phys. Rev. Lett. **117** 102501 (2016).
- Y. Togano et al., Phys. Lett. B **761** 412-418 (2016).
- H. T. Fortune, Phys. Rev. C **94** 064307 (2016).

Carbon isotopes $^{10-22}\mathrm{C}$ properties

Quadrupole deformation of carbon isotopes:

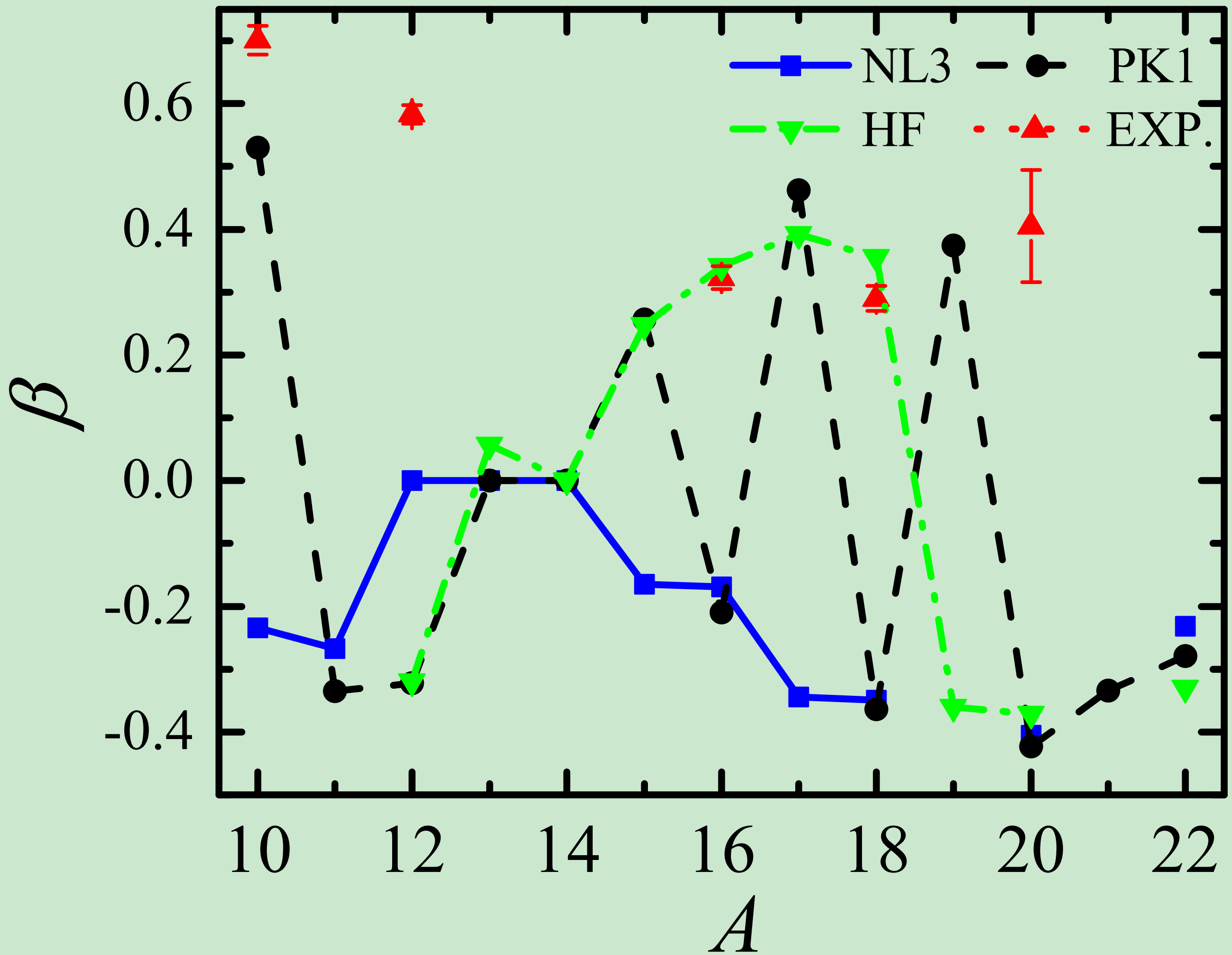

The experimental data are taken from

B.Pritychenko et al., Atomic Data and Nuclear Data Tables **107** 1 (2016).

^{22}C: Halo structure

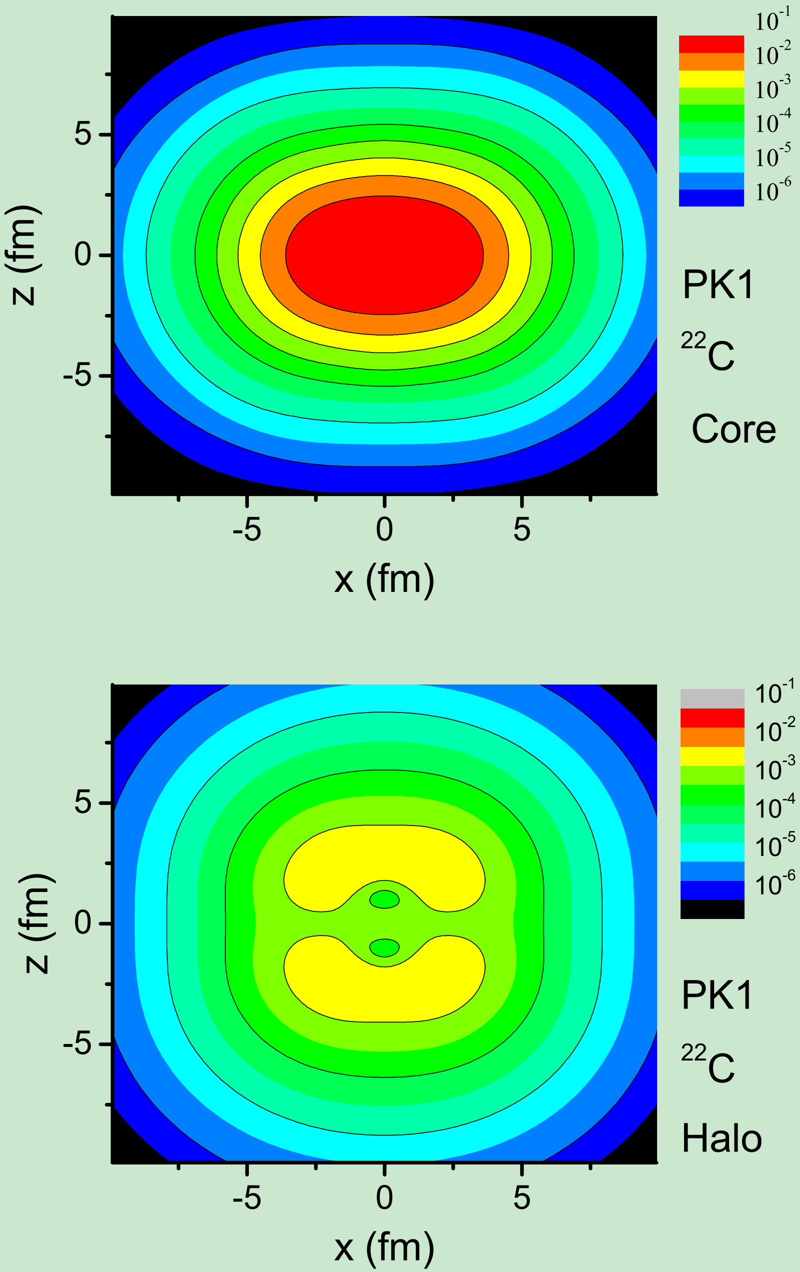

PK1: $R_m = 3.24$ fm, $\beta_{20} = -0.28$, $S_{2n} = 0.84$ MeV.

Exp.: $R_m = 3.44 \pm 0.08$ fm, $S_{2n} = 0.42 \pm 0.94$ MeV.

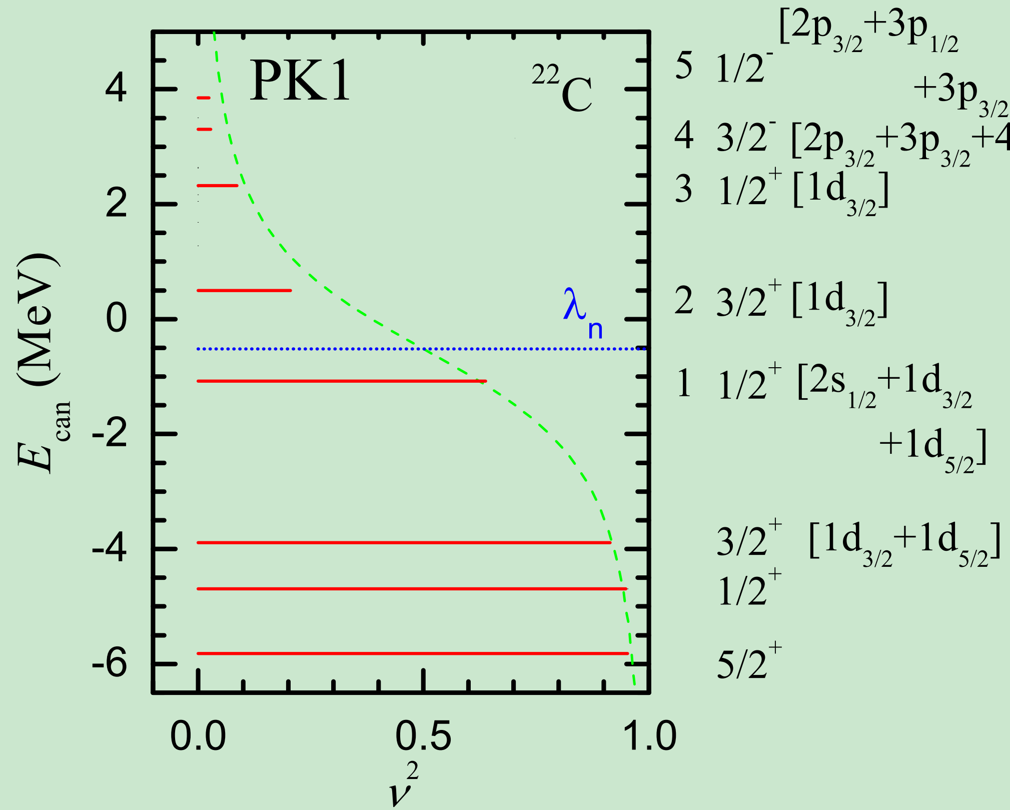

Core: $E_{\mathrm{can}} < -3$ MeV; Halo: $E_{\mathrm{can}} > -2$ MeV.

^{22}C: Halo structure

$$f(\mathbf{r}) = \sum_\lambda f_\lambda(r)P_\lambda(\cos\theta),\ f_\lambda(r) = \frac{2\lambda+1}{2}\int_{-1}^{1} d(\cos\theta) f(\mathbf{r})P_\lambda(\cos\theta),\ \lambda = 0, 2, 4\ldots$$

Spherical, quadrupole and hexadecapole component of core density.

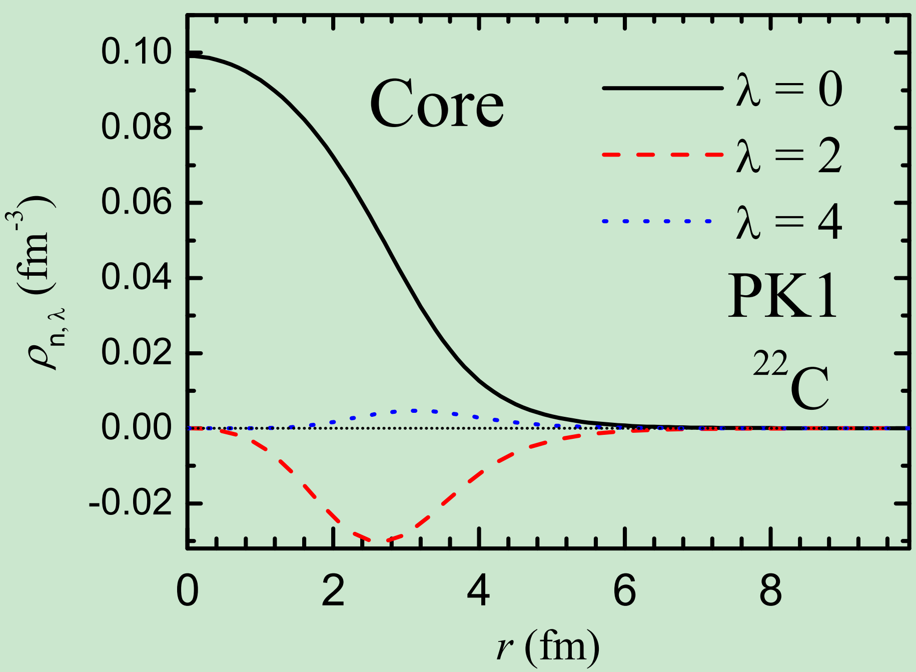

oblate core

Spherical, quadrupole and hexadecapole component of halo density.

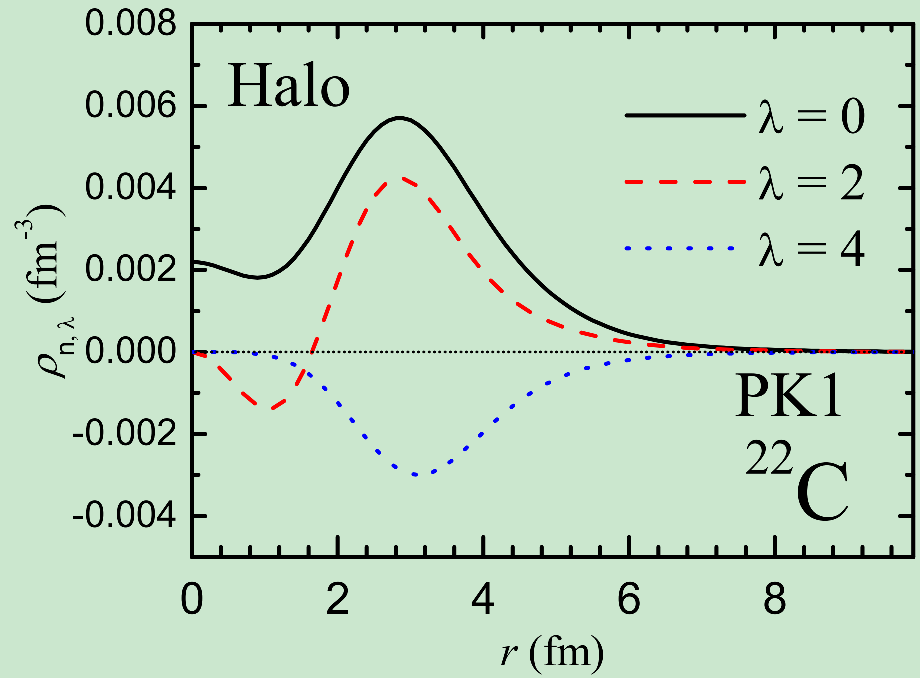

prolate halo

^{22}C: Halo structure

Total density, Core and halo, neutron orbitals.

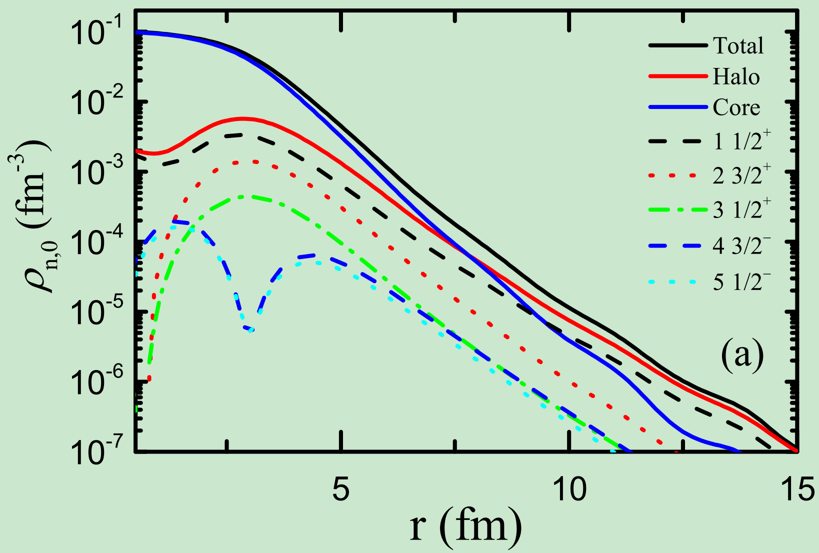

(1-$\frac{1}{2}^{+}$) near the fermi surface gives a most contribution the halo of ^{22}C.

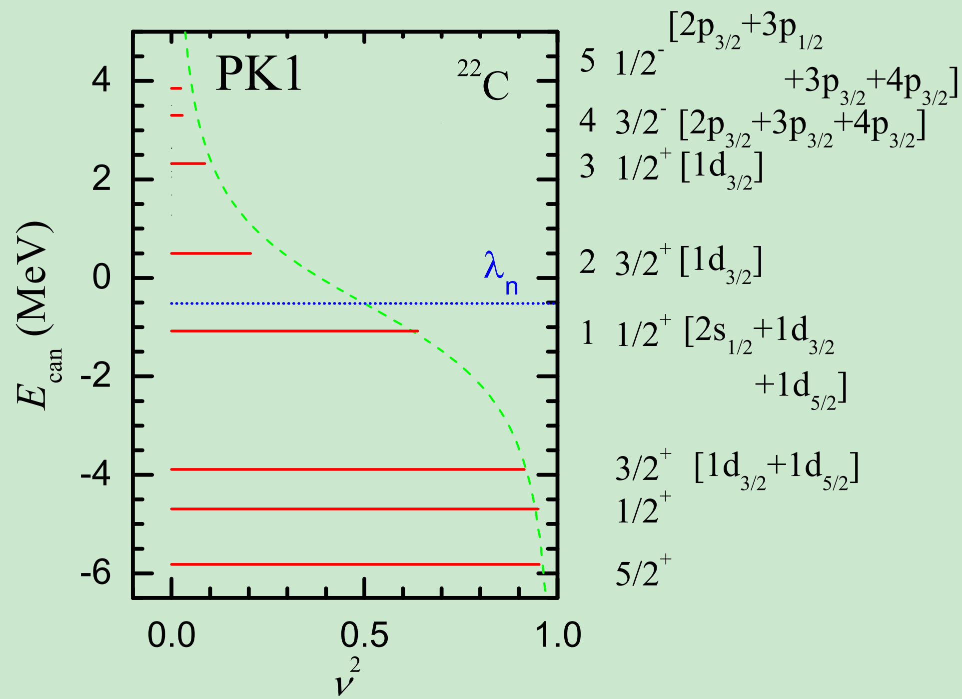

Relative contribution of neutron orbitals to total density.

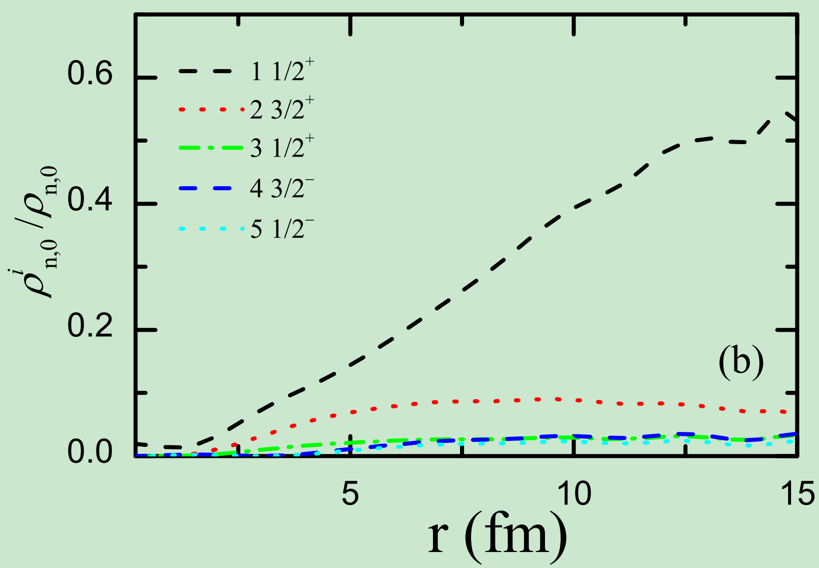

Spherical components   low j(s, p)-orbitals

$2s_{1/2}$(0.13/0.63): spherical halo;

$1d_{5/2}$(0.45/0.63): prolate shape for halo.

Constraint calculation of ^{22}C

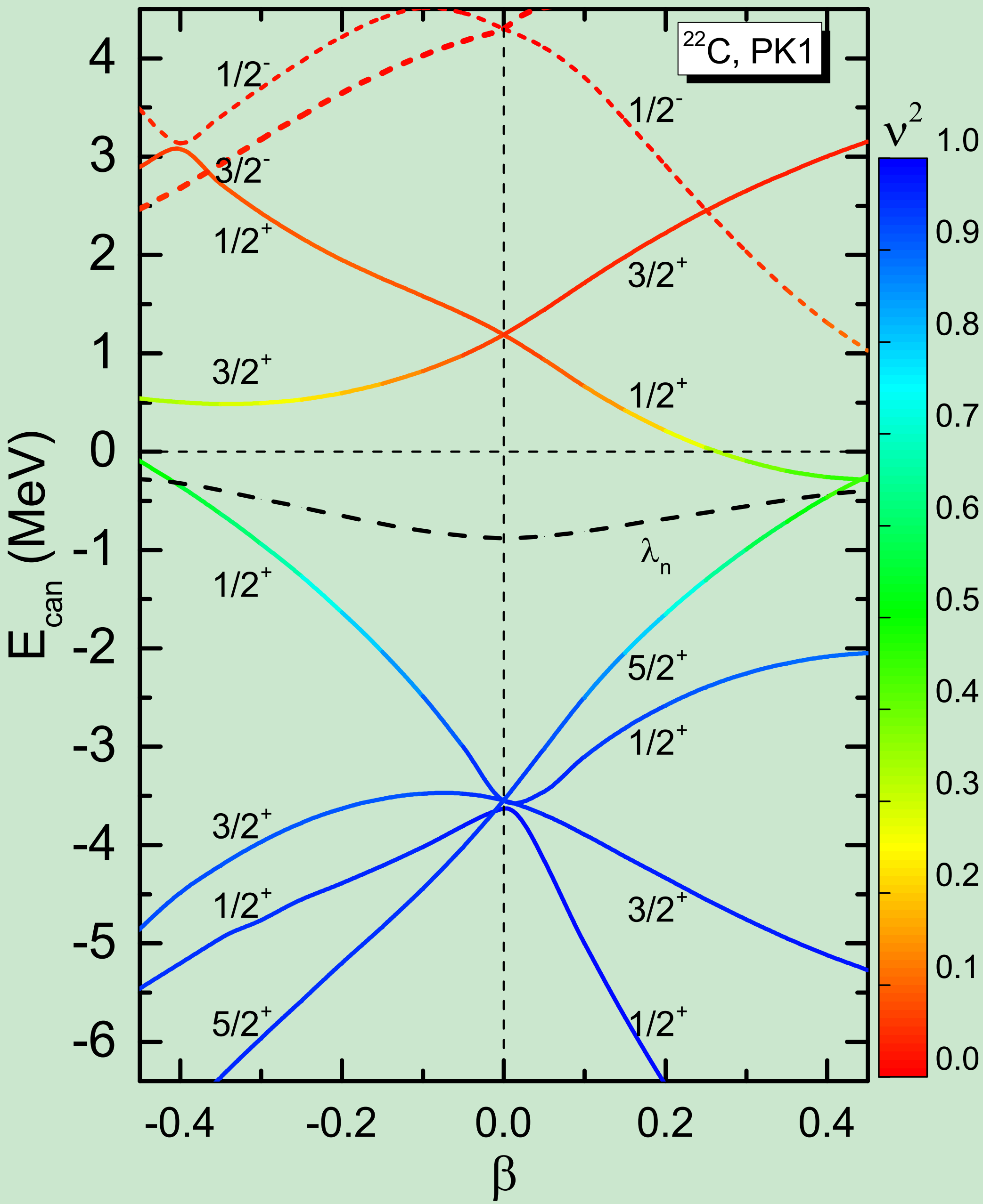

Constraint calculation of ^{22}C

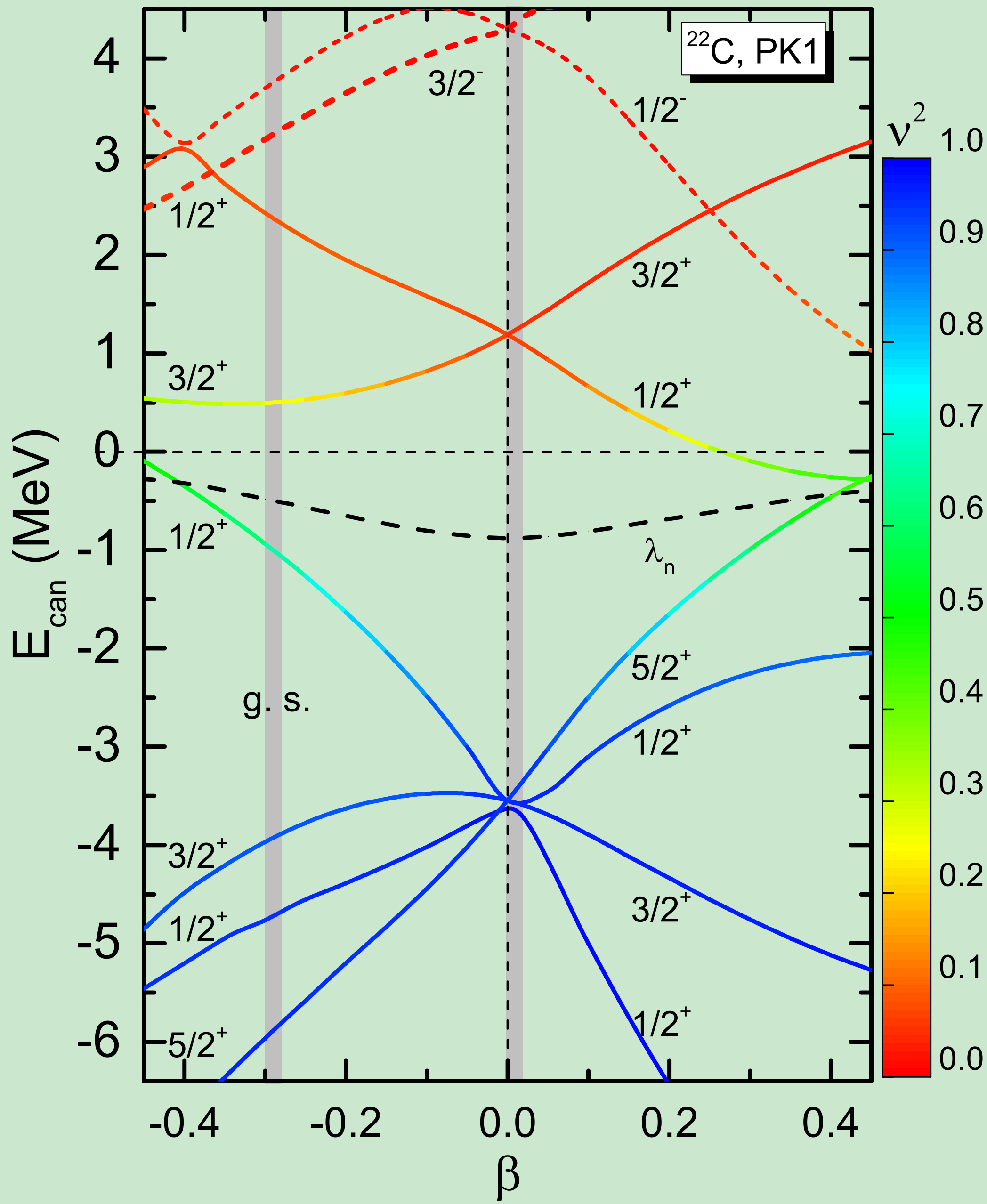

Constraint calculation of ^{22}C

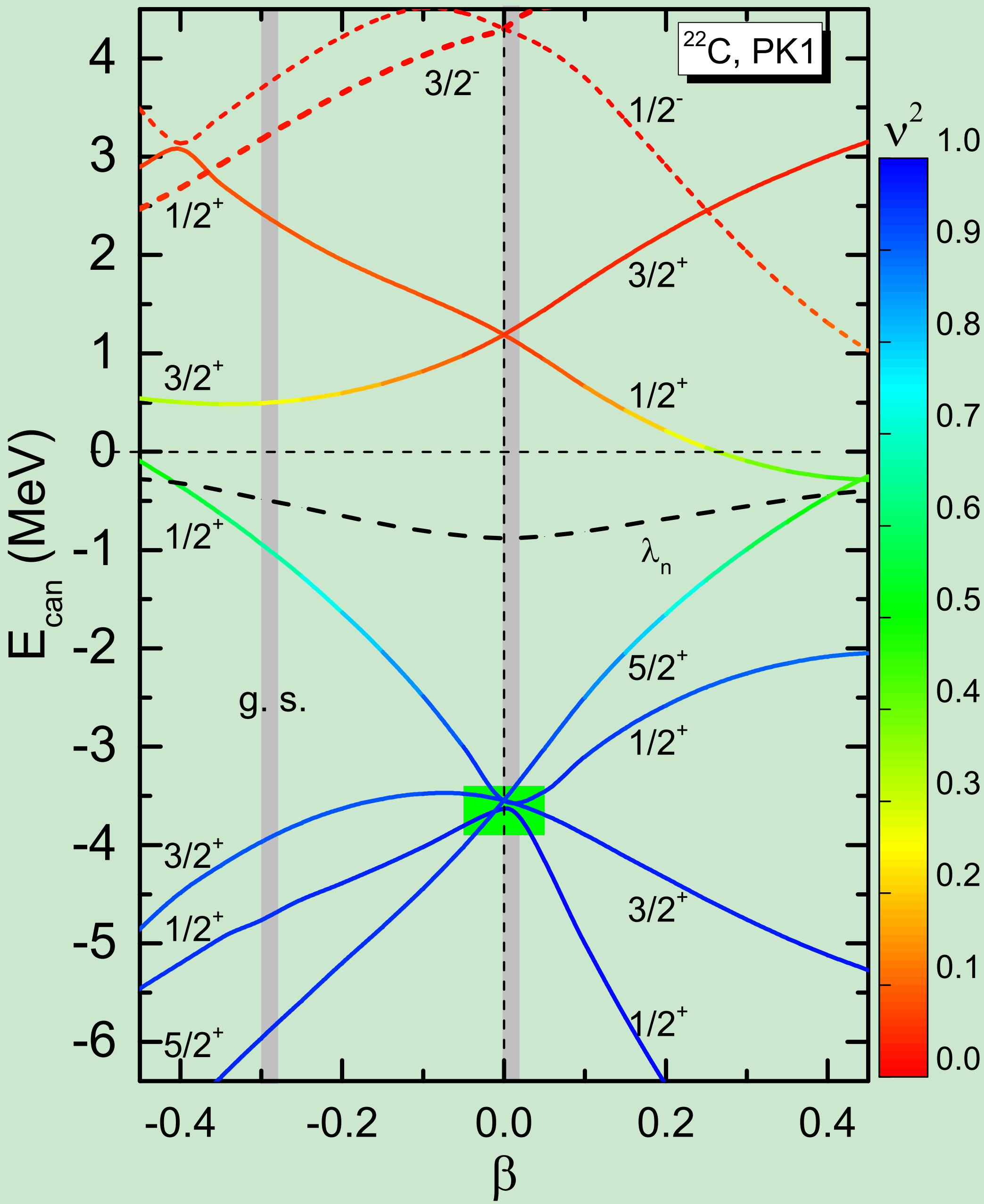

Constraint calculation of ^{22}C

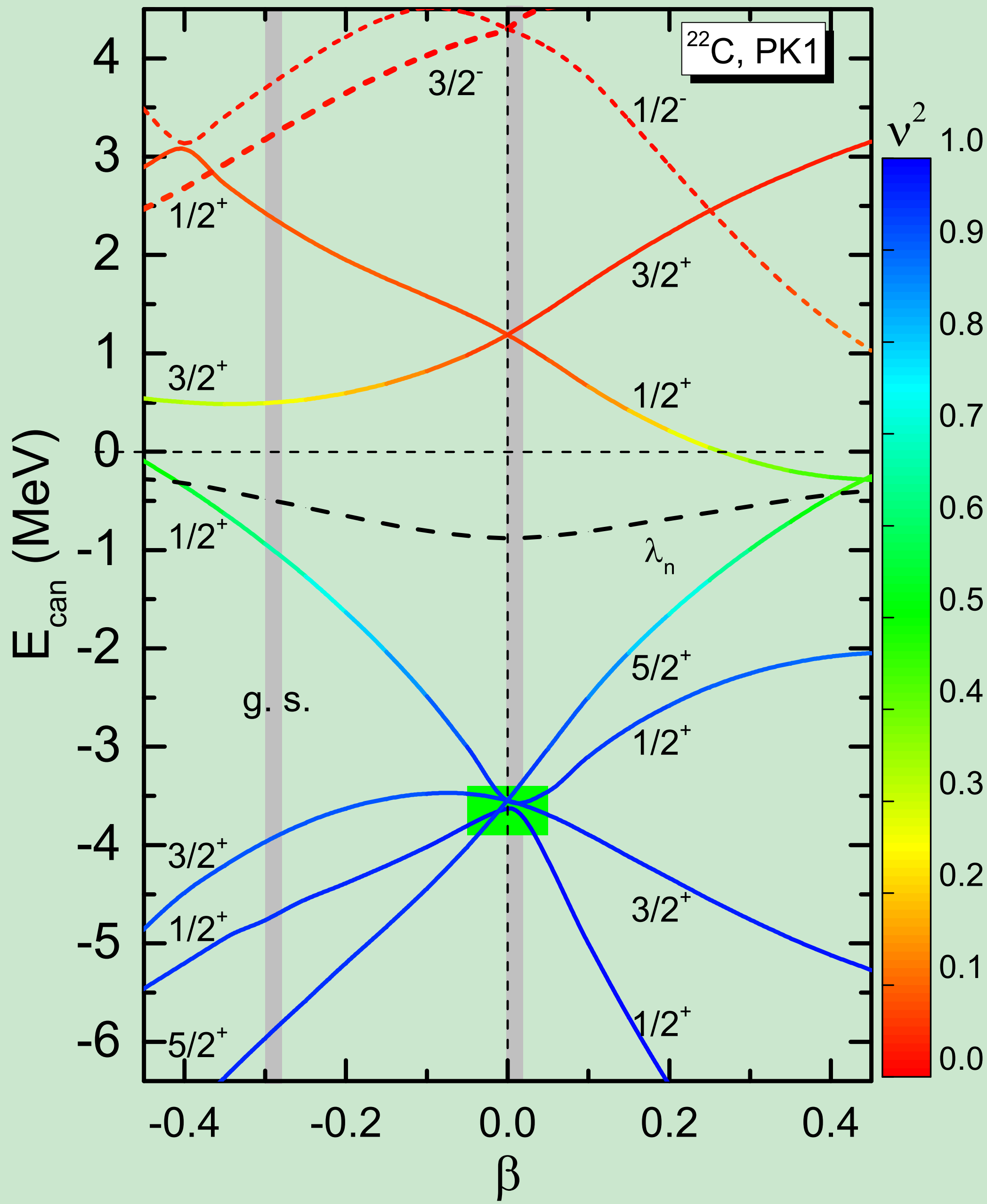

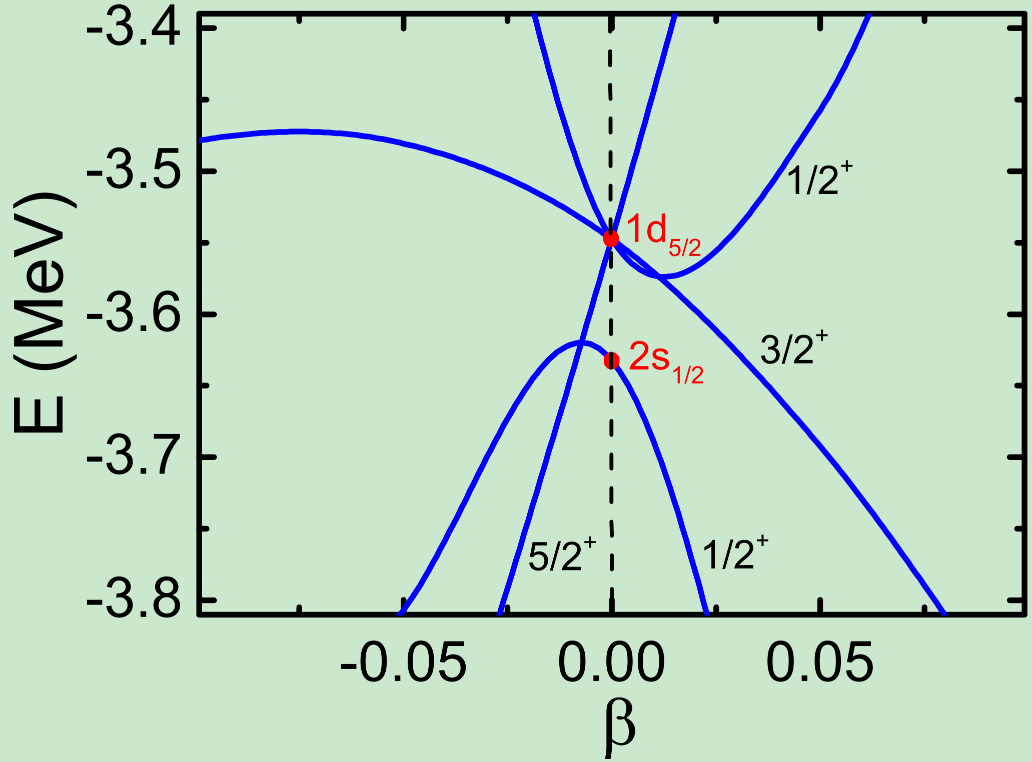

$2s_{1/2}$ is lower than $1d_{5/2}$. ^{11}Li, ^{11}Be, and ^{14}Be, the mixing of $(2s_{1/2})^2$ and $(1p_{1/2})^2$.

- A. Ozawa, et al, Phys. Rev. Lett. **84**, 5493 (2000)
- Takaharu Otsuka, et al, Phys. Rev. Lett. **87**, 082502 (2001)

OUTLINE

Summary

- Description of the bulk properties of Carbon isotopes with DRHBc model.
- The deformed halo structure of $^{22}\mathrm{C}$.
  1. Deformation effect is important for the ^{22}C halo;
  2. shape decoupling: oblate core and prolate halo;
  3. The main contribution of the halo is the $\frac{1}{2}^{+}$ level close to fermi surface, whose main spherical components are $2s_{1/2}$, $1d_{5/2}$ and $1d_{3/2}$ with the amplitude of 0.14, 0.43, and 0.06;
  4. Orbitals with low j orbitals, $2s_{1/2}$ component give a spherical halo, gives the halo structure of ^{22}C, but a large component of $1d_{5/2}$ leads to a prolate shape.
  5. $2s_{1/2}$ is lower than $1d_{5/2}$, so the percentage of $2s_{1/2}$ is only about 20% for the valence neutron orbitals.

Thanks for your attention.